

Preparation and evaluation of the cytotoxic nature of TiO₂ nanoparticles by direct contact method

M Chellappa¹
U Anjaneyulu¹
Geetha Manivasagam²
U Vijayalakshmi¹

¹School of Advanced Sciences,
Materials Chemistry Division,

²Centre for Biomaterials Science
and Technology, School of Mechanical
and Building Sciences, VIT University,
Vellore, Tamil Nadu, India

Abstract: The purpose of this study is to prepare and evaluate the effect of synthesized titanium dioxide (TiO₂) nanoparticles for their biocompatibility on physiological body fluids and the effect of cell toxicity to produce osteointegration when used as implantable materials. For the past few decades, the number of researches done to understand the importance of the biocompatibility of bioceramics, metals, and polymers and their effect on clinical settings of biomedical devices has increased. Hence, the total concept of biocompatibility encourages researchers to actively engage in the investigation of the most compatible materials in living systems by analyzing them using suitable physical, chemical, and biological (bioassay) methods. The ceramic material nano TiO₂ was prepared by sol-gel method and analyzed for its functional group and phase formation by Fourier transform infrared spectroscopy and powder X-ray diffraction. Furthermore, the particle size, shape, surface topography, and morphological behavior were analyzed by dynamic light scattering, zeta potential, scanning electron microscopy–energy dispersive X-ray analysis, and transmission electron microscopy analysis. In addition to this, the cytotoxicity and cytocompatibility were determined on MG63 cell lines with varying doses of concentrations such as 1 µg/mL, 10 µg/mL, 25 µg/mL, 50 µg/mL, and 100 µg/mL with different time periods such as 24 hours and 48 hours. The results have not shown any toxicity, whereas, it improved the cell viability/proliferation at various concentrations. Hence, these findings indicate that the nano TiO₂ material acts as a good implantable material when used in the biomedical field as a prime surface-modifying agent.

Keywords: biomaterial, implant, biocompatible, MTT assay, osteointegration, MG63 cell lines

Introduction

Biomaterials with specific structural and functional characteristics, including metals, ceramics, and polymers, have been used in biomedical devices as drug delivery devices and as implantable prostheses to elicit intimate contact with biological systems of cells and proteins.¹ The advancement in science and nanotechnology has produced abundant biomaterials with specific intriguing physicochemical and biological properties such as improved surface topography, nanoscale and microscale particle size distribution, and different phase compositions with improved biocompatibility. Hence, these materials should possess increased wear and mechanical strength with superior corrosion-resistant properties to fulfill the requirements for biomedical applications.^{2–4}

The farthestmost requirement for better efficacy of biomaterial is its biocompatible nature with the host tissue upon implantation. The clinical success of a biomaterial depends upon the ability to produce the required effect of cellular or tissue response.

Correspondence: U Vijayalakshmi
School of Advanced Sciences, Materials
Chemistry Division, VIT University,
Vellore 632 014, Tamil Nadu, India
Email vijayalakshmi.u@vit.ac.in

In addition to the cellular effect, cytotoxicity, genotoxicity, mutagenicity, carcinogenicity, and immunogenicity are also components of biocompatibility, and this must be evaluated or studied as prescreening tests by in vitro cell culture methods, to justify overall cell viability of a biomaterial, which is the most important factor for the bioactive effect of implants and prostheses.⁵⁻⁷ The best cell crawl of a prepared biomaterial should not have any stress or toxicity to cells and should be therapeutically acceptable with enhanced mobilization, as well as more activity with more visible diagnostic characteristics. These characteristics depend on the site of implantation, the required function and size, and the host-implant interaction over the established period.⁸ It is well known that ceramic biomaterials are collectively a group of ceramics, chemically an inorganic substance, used for repairing living tissues and organs and for the replacement of diseased and damaged parts of the human body such as in the musculoskeletal system, cardiovascular system, organs and senses, hip replacements, prosthetic heart valves, dental implants, and orthopedic prostheses. Materials such as metals and their alloys, polymers, ceramics, and composites are widely used in biomaterials. Bioceramics encounter different physicochemical properties in the human body, such as complex interaction/reaction with tissues and cells, which can lead to failure or toxicity.^{9,10} For the past few decades, a number of in vitro and in vivo studies have been carried out with more models of human and rodent cell lines, bacteria, yeast, and fresh water algae.¹¹⁻¹³ St Pierre et al¹⁴ studied osteolysis by the stimulation of NALP3 inflammasome and recruitment of neutrophils with inflammatory response due to generation of debris from titanium implants after total hip replacements by using TiO₂ particles. Xiong et al¹⁵ also discussed the effect of particle size on the cytotoxicity of polylactic-co-glycolic acid (PLGA), TiO₂ composite, and the adverse effects on RAW264.7 and BEAS-2B cells. In addition to that, the wide industrial applications of the nanoparticles is concerning and makes it essential to test its potential toxicity in different cell lines. Sayes et al¹⁶ studied the decreased toxicity of the rutile form of TiO₂ on A549 cells. Another study by Wang et al¹⁷ confirmed the toxicity of titanium particles on knee joints in a rabbit model due to DNA damage by oxidative catalyze. Based on the results of these studies, TiO₂ particles exhibit low-to-moderate toxicity due to the physical, chemical, and biological properties of nanomaterials.

TiO₂ has been increasingly used for its good fatigue strength, resistance to corrosion, better biocompatibility, and photocatalytic property.¹⁸ These ubiquitous application

properties naturally exist in TiO₂ powder because it is inert and thermally stable with noninflammable characteristics due to different polymorphic forms of anatase, rutile, brookite and oxygen deficient α -Ti₃O₅. The anatase and brookite forms are less stable and transform to a stable rutile form depending on the processing conditions such as heating temperature and environmental conditions, thereby altering the particle size. The particle size has to be evaluated due to the fact that the nanomaterials have specific properties such as the largest surface area with a smaller particle size and shape, which exhibits different biocompatibility or sometimes toxicity than the micro-sized particles.^{19,20} TiO₂ nanoparticles have wide industrial applications, such as in pharmaceuticals, pigments, and cosmetics, and particularly wide usage in the biomedical field as an integrating agent to bone tissue. However, the toxicity of TiO₂ is unclear and it has to be evaluated on implant and prostheses for better application. The material toxicity to human beings is acute and chronic and direct and indirect; various types of local and systemic toxicity must be separately validated by systematic in vitro and in vivo methods.^{21,22} Consistent with the findings of the literature survey, a limited number of in vitro biocompatibility studies using osteoblast cell lines were carried out for TiO₂ nanoparticles for bone tissue applications.²³ Hence, in this paper, we report the preparation of TiO₂ by sol-gel method with novel characteristic properties of nanosize particles with 100% rutile polymorphic nature. The synthesized materials have been evaluated for the presence of functional groups, phase formation, and morphological features by Fourier transform infrared spectroscopy (FT-IR), Powder X-ray diffraction (XRD), scanning electron microscopy (SEM)-energy dispersive X-ray analysis (EDAX), dynamic light scattering (DLS), zeta potential, and transmission electron microscopy (TEM) analysis. The in vitro cytocompatibility test has been carried out using the MTT assay (3-[4,5-dimethylthiazol-2-yl]-2,5-diphenyl tetrazolium bromide) as a basic screening method. The so-called MTT colorimetric method involves coloration of cells by MTT dye. This mitochondrial activity method has unique properties such as simplicity, sensitivity, and reliability, and it is also possible to test any level of toxic effect on cell lines and is thereby easily assessable for in vivo animal studies.

Materials and methods

Preparation of titanium dioxide nanoparticles

TiO₂ nanoparticles were prepared by using pure titanium (IV) isopropoxide as a precursor. The titania precursor,

glacial acetic acid, and double-distilled water were mixed at a molar ratio of 1:30:300 under constant stirring conditions for 2 hours at room temperature. The resultant mixture was transferred to a round-bottom flask fitted with reflux condenser and was refluxed in an oil bath at a controlled temperature of 70°C for 12 hours with constant stirring. The sol was evaporated in a water bath and the obtained precipitate gel was dried in an oven for 2 hours at 100°C . Finally, it was sintered at 900°C for 2 hours at a heating rate of $1^\circ\text{C}/\text{min}$. The obtained TiO_2 nanoparticles were characterized for phase purity, particle size, shape, and elemental analysis. The experimental procedure carried out to synthesize TiO_2 nanoparticles is depicted as a flow chart in Figure 1.

Biocompatibility test

Mitochondrial activity (principle)

The proliferation and viability of the prepared nano TiO_2 particles were assessed on human osteoblast cell-like MG63 cell lines using the MTT colorimetric assay. This cell line is an appropriate primary cell line used to understand the biocompatibility and bone cell induction. The assay is based on the reduction of soluble yellow tetrazolium salt to blue-colored insoluble formazan crystals by metabolically

active cells. Only live cells are able to take up the tetrazolium salt. The enzyme mitochondrial dehydrogenase present in the mitochondria of the live cells is able to convert internalized tetrazolium salt to formazan crystals, which are blue in color. Then the cells are lysed and dissolved in dimethyl sulfoxide (DMSO) solvent. The quantity of blue-colored insoluble formazan formed is proportional to the number of cells involved in the process. By measuring the intensity of light, we can determine indirectly the number of cells involved in the reaction. The color development is then determined in an ELISA reader at 570 nm. From this study, the cellular activity and proliferation of cells or toxicity should be determined for the prepared sample to examine the biocompatibility.

Cell culture procedure

The compound was dissolved in 10% DMSO to give a final concentration of DMSO not more than 0.5% and should not affect the cell survival. The MG63 cell lines were plated separately in 96-well plates at a concentration of 1×10^5 cells/well. After 24 hours, cells were washed twice with 100 μL of serum-free medium and starved for 1 hour at 37°C . After starvation, the cells were treated for the investigation of dose-dependent as well as time-dependent effects of prepared TiO_2 nanoparticles. Different doses of test compounds (1 $\mu\text{g}/\text{mL}$, 10 $\mu\text{g}/\text{mL}$, 25 $\mu\text{g}/\text{mL}$, 50 $\mu\text{g}/\text{mL}$, and 100 $\mu\text{g}/\text{mL}$) are incubated for different time periods such as 24 hours and 48 hours. At the end of the treatment period, the medium was aspirated and serum-free medium containing MTT (0.5 mg/mL) was added and incubated for 4 hours at 37°C in a CO_2 incubator. The 50% inhibitory concentration value of the crude extracts was identified in a normal osteoblast cell line.

The MTT-containing medium was then discarded, and the cells were washed with 200 μL of phosphate-buffered saline with pH 7.4. The crystals were then dissolved by adding 100 μL of DMSO, and this was mixed properly by pipetting up and down. Spectrophotometrical absorbance of the blue-colored insoluble formazan was measured in a microplate reader at 570 nm (Bio-Rad 680). Cytotoxicity was determined using GraphPad Prism 5 software.

Characterization techniques

FT-IR spectra

The functional characteristics of TiO_2 were determined by FT-IR spectroscopy in the range of $400\text{--}4,000\text{ cm}^{-1}$ using a Shimadzu model 8300 spectrophotometer by using a KBr pellet technique (0.1 weight%).

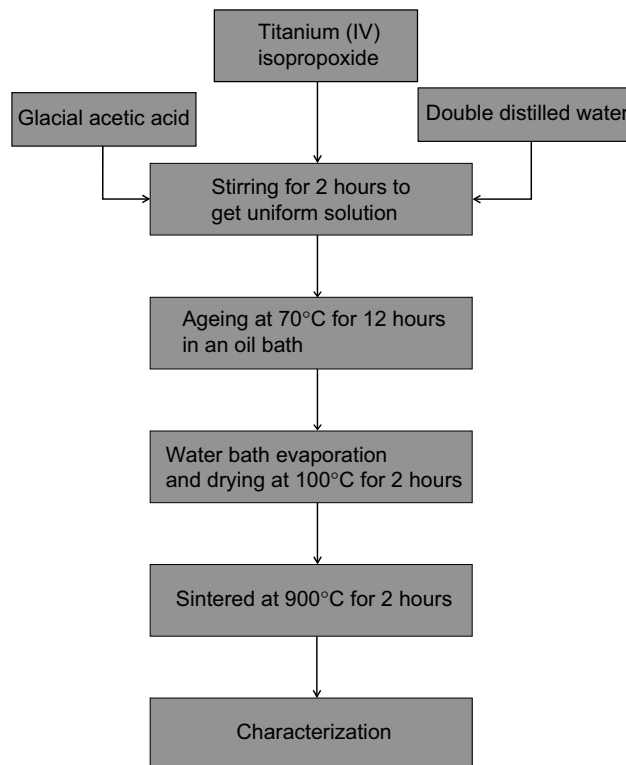


Figure 1 Flow chart for the synthesis of TiO_2 nanoparticles from Titanium (IV) isopropoxide via sol-gel process.

Abbreviation: TiO_2 , titanium dioxide.

XRD analysis

The XRD patterns were recorded in an X-ray diffractometer (D8 model, Bruker, Germany) with a step size of 0.02° and a scan rate of $1^\circ/\text{min}$ with Cu $K\alpha$ radiation ($\lambda=1.54056 \text{ \AA}$). The fraction of crystallinity, crystallite size, and specific surface area of the prepared nano TiO_2 particles were also assessed from the study. The crystallite size was calculated using Scherrer's formula²⁴:

$$D = K\lambda/\beta\cos\theta$$

where D is the crystal size, K is Scherrer's constant usually taken as 0.89, λ is the X-ray wavelength of Cu $K\alpha$ radiation ($\lambda=1.54056 \text{ \AA}$), β is the line width of half maximum in radians, and θ is Bragg's diffraction angle. The fraction of crystallinity was obtained using the following formula:

$$X_c = (0.24/\beta)^3$$

Specific surface area of the prepared TiO_2 nanoparticles was also obtained using formula:

$$S = 6 \times 10^3 / d\rho$$

where d is the theoretical density of TiO_2 particles (anatase 3.894 g/cm^3 and rutile 4.25 g/cm^3) and ρ is the crystallite size (nm).

Scanning electron microscopy–EDAX

The prepared TiO_2 nanoparticles were subjected to SEM-EDAX analysis for the chemical constituent changes occurred on the surface. The instrument Philips 501 SEM equipped with X-ray microanalysis was used for the determination of microstructural (surface topography) and elemental analysis of the powder sample.

TEM analysis

The TEM measurements were recorded to determine the primary particle size distribution in the prepared TiO_2 nanoparticles sintered at 900°C for 2 hours using TEM: Tecnai20G2FEI (the Netherlands). The diffraction pattern of the selected area in the sample study was also placed as inset into the TEM image to understand the crystallite size and lattice pattern.

Dynamic light scattering

DLS measurements of the prepared TiO_2 were performed using the high-performance particle size analyzer Malvern Zetasizer by dispersing appropriate concentration of powder

such as 0.01 g/100 mL in DMSO. The same medium was adopted to predict the cytotoxicity analysis upon dispersion of particles in DMSO.

Zeta potential

The zeta potential (ξ) was based on the surface charge of the particles relative to the local environment of the prepared particle. This electrostatic potential of shear plane of the particle was carried out in ultrasonicated dispersion of 0.01 g/100 mL in DMSO in room temperature using the Horiba SZ-100 nanoparticle analyzer.

Results

FT-IR spectral analysis

FT-IR spectral analysis is an imperative as well as an intriguing technique to predict the formation of functional groups in the prepared TiO_2 nanoparticles. The characteristic absorption of raw and sintered sample differs from their relative intensity of peaks and the reduction in number of peaks with respect to the sintering temperature (Figure 2). The formation of nano TiO_2 was confirmed by the characteristic peaks observed at $2,926 \text{ cm}^{-1}$, $1,641 \text{ cm}^{-1}$, and $1,157 \text{ cm}^{-1}$ in the sintered sample. The peaks at $1,400 \text{ cm}^{-1}$ and $1,529 \text{ cm}^{-1}$ correspond to symmetric and asymmetric stretching vibrations of the adsorbed acetic acid, carboxylic group co-ordinating to Ti. Hydroxyl peak intensity at $3,600\text{--}3,100 \text{ cm}^{-1}$ and $1,630\text{--}1,620 \text{ cm}^{-1}$ was found to be decreased with an increase in sintering temperature, which indicates the removal of large portions of adsorbed water from raw TiO_2 . Also the broad, intense band below $1,000 \text{ cm}^{-1}$ in the raw spectrum is due to Ti-O-Ti vibrations, to which the formation of TiO_2 is attributed. The mixture of

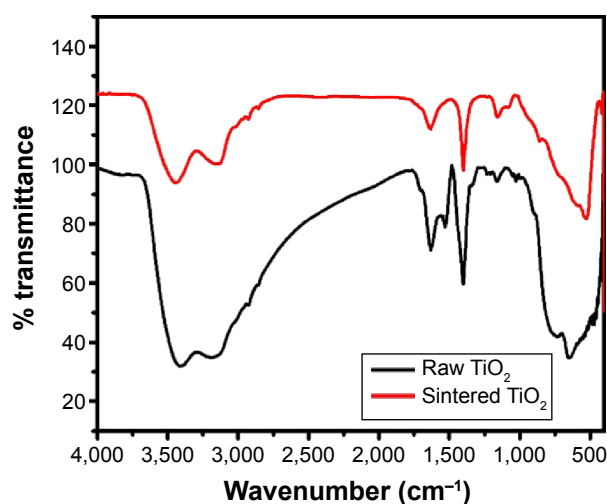


Figure 2 FT-IR spectra for raw and sintered TiO_2 nanoparticles at 900°C for 2 hours.

Abbreviations: FT-IR, Fourier transform infrared spectroscopy; TiO_2 , titanium dioxide.

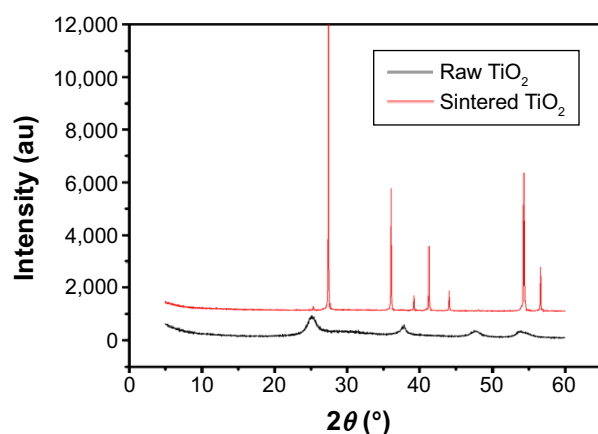


Figure 3 XRD pattern of raw and sintered TiO₂ nanoparticles at 900°C for 2 hours.
Abbreviations: XRD, X-ray diffraction; TiO₂, titanium dioxide.

polymorphic phases of anatase and rutile was observed from 400–800 cm⁻¹ in the raw powder and transformed into 100% rutile phase at a sintering temperature of 900°C, which corroborates with previous studies.^{25,26}

XRD analysis

The formation of phases, fraction of crystallinity, crystallite size, and specific surface area for the prepared TiO₂ nanoparticles before and after sintering at a temperature of 900°C for 2 hours was confirmed by XRD analysis (Figure 3). The XRD pattern of raw TiO₂ shows a characteristic diffraction peak with 2θ values lying at 2θ=25.23° (101), 2θ=37.9° (004), 2θ=47.57° (200), and 2θ=53.53° (105) corresponds to anatase phase and is confirmed with Joint Committee on Powder Diffraction Standards [JCPDS] [01 078 2486]. The presence of a broad base line as well as a broad diffraction line indicates the presence of small amounts of amorphous phase with nanosize crystallites, respectively.

The characteristic peaks in the sintered sample at 2θ=27.45° (110), 2θ=36.08° (101), 2θ=41.25° (111), 2θ=54.34° (211), and 2θ=56.66° (220) correspond to rutile phases of TiO₂ and are further confirmed with JCPDS (01 087 0710). From the spectrum, it was observed that all the peaks correspond to rutile phase, and there was a phase transformation from anatase to rutile phase in nano TiO₂ when heat

treatment was given at higher temperatures, and all the peaks in the prepared TiO₂ nanoparticles exactly matched with the software.^{27,28} The presence of sharp diffraction peaks in the sintered sample indicates high purity, nanosize, and more crystalline nature of the prepared TiO₂ nanoparticles. The phases, fraction of crystallinity, crystallite size, and specific surface area formed in the prepared TiO₂ nanoparticles before and after sintering are tabulated in Table 1. The sintering process at 900°C for 2 hours produces prime changes compared with the unsintered one such as an increase in crystallite size of 114 nm, better fraction of crystallinity of 28.1450 with decreased specific surface area of 12 m²/g, and 100% pure rutile phase transformation. The increase in crystallinity of the sintered sample should be more useful in the stability of prepared suspension for better biological analysis.

Scanning electron microscopy with EDAX

The surface morphology as well as the particle size of the pure TiO₂ nanoparticles sintered at 900°C for 2 hours are shown in Figure 4. The images clearly show agglomerated platelet-like particle distribution throughout the study.^{29,30} The sintering process produces grain growth and agglomeration between the particles with an average particle size of 76 nm.

The elemental compositions of sintered TiO₂ nanoparticles at 900°C for 2 hours were confirmed by EDAX analysis (Figure 5). The elemental composition profile indicates two peaks approximately 0.2 keV and 4.5 keV, respectively. The less intense peak is assigned to the surface TiO₂ and the more intense one to the bulk TiO₂. The peaks of “O” radical are also distinct at 0.5 keV. The quantitative measurements of all the elements present in the sintered sample are shown in Table 2.

TEM analysis

The particle size and shape of the TiO₂ nanoparticles sintered at 900°C for 2 hours were characterized by TEM analysis and the results are shown in Figure 6. The presence of a nonhomogeneous structure with agglomeration of particles is clearly seen from the analysis. The decreased distribution of spherical shaped particles with more platelet-like particles of different sizes corroborates with SEM analysis.

Table 1 Line width, crystallite size, fraction of crystallinity, specific surface area, anatase, and rutile forms of sintered TiO₂ nanoparticles at 900°C for 2 hours

Plane	Line width (FWHM)	2θ	Crystallite size (D) nm	Fraction of crystallinity X _c	Specific surface area, S (m ² /g)	Anatase %	Rutile %
101 (raw sample)	1.4198	25.23	5	0.00483	308	100	—
110 (sintered sample)	0.0789	27.45	114	28.1450	12	—	100

Abbreviations: FWHM, full width at half maximum; TiO₂, titanium dioxide.

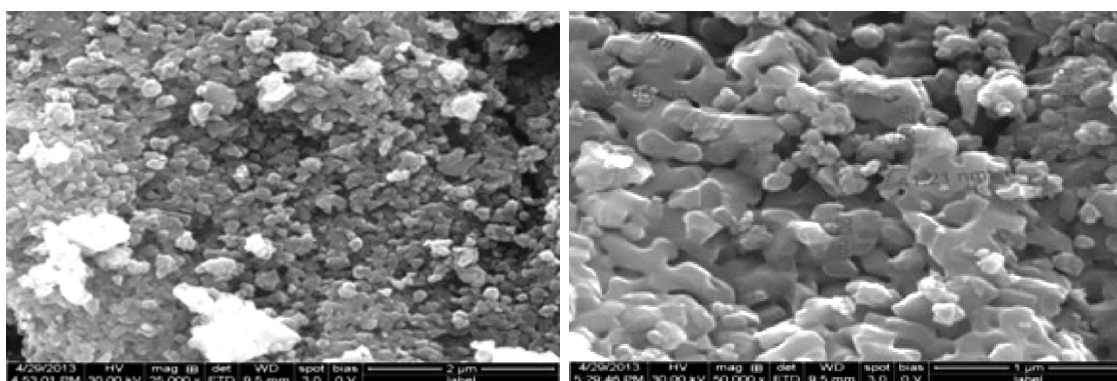


Figure 4 SEM images of TiO₂ powder sintered at 900°C for 2 hours (different magnification).

Abbreviations: SEM, scanning electron microscope; TiO₂, titanium dioxide.

The selected area electron diffraction (SAED) pattern of inset clearly indicates the crystalline nature of the prepared TiO₂ nanoparticles. The average particle size in the range of 125 nm studied by TEM analysis is consistent with SEM and XRD analysis.

DLS and zeta potential

The experimental values of DLS analysis as well as zeta potential of prepared TiO₂ nanoparticles sintered at 900°C for 2 hours are shown in Figures 7 and 8, respectively. DLS study has been used to understand the nature of hydrodynamic size (diameter) of prepared TiO₂ nanoparticles in DMSO. The study shows a fairly small agglomeration with average hydrodynamic diameter of 1,140 nm with Pdi value of 0.158.

The zeta potential with a positive value of 26.8 mV with electrophoretic mobility 0.000056 cm²/Vs was obtained for the TiO₂ nanoparticle suspension in DMSO, which clearly indicates a stable dispersion without particle settlement. Furthermore, the study of prepared suspension corroborates with

general criteria of zeta potential (ξ) value 30 mV with positive or negative sign for better stability. Zhang et al³¹ confirmed the measurement of zeta potential of the material to understand the nature of cellular interaction, cellular diagnostics, and therapeutics of normal and cancer cell effects.

Biocompatibility test (cytotoxicity)

The viability/proliferation of osteoblast-like MG63 cell lines was studied using MTT assay for TiO₂ at various doses of concentrations, 1 µg/mL, 10 µg/mL, 25 µg/mL, 50 µg/mL, and 100 µg/mL for 24 hours and 48 hours. The increased viability and cell proliferation of MG63 cell lines were confirmed and the morphological features of control and treated cell lines were described with the help of the phase contrast microscope (Figures 9 and 10).

The percentage of viability/proliferation of cells with respective concentration is shown in Figure 11. The cell viability/proliferation of the sample compared to control (without TiO₂) has not shown any potential cytotoxicity at concentrations of 25 µg/mL, 50 µg/mL, and 100 µg/mL for 48 hours. In low concentrations with short time periods, there was a smaller increase in cell activity. Furthermore, the parameters such as concentration, method of preparation of nanoparticles, and structure have an influence on osteoblast cell viability, which was further proved by Nathanael et al.³² In their study, the composites made of hydroxyapatite (HAP)

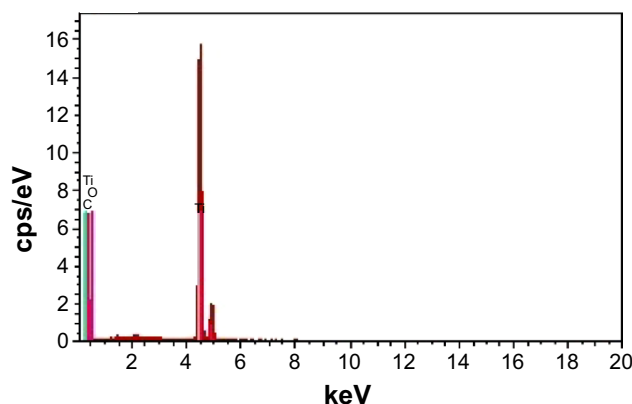


Figure 5 Energy dispersive X-ray analysis spectrums of TiO₂ powder sintered at 900°C for 2 hours.

Abbreviation: TiO₂, titanium dioxide.

Table 2 EDAX analysis of sintered TiO₂ nanoparticles at 900°C for 2 hours

Element	Wt%	At%
TiK	44.37	20.79
O	53.00	74.30
C	2.63	4.92

Abbreviations: EDAX, Energy dispersive X-ray analysis; TiO₂, titanium dioxide.

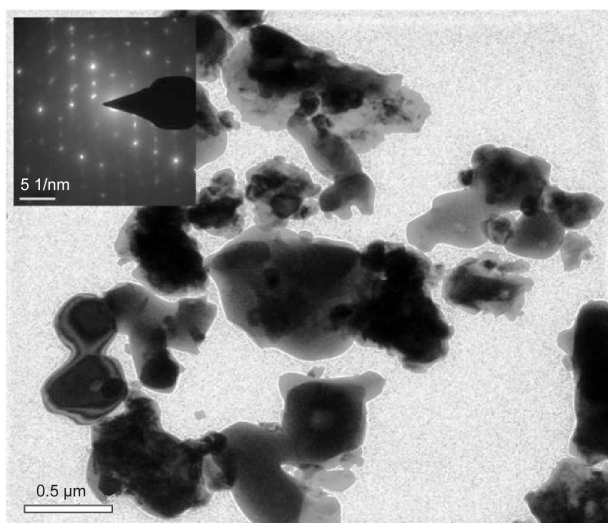


Figure 6 TEM images of TiO₂ powder sintered at 900°C for 2 hours (insets: SAED patterns).

Abbreviations: TEM, transmission electron microscope; TiO₂, titanium dioxide; SAED, selected area electron diffraction.

and TiO₂ have a greater change in cellular response with respect to concentration on osteoblast-like Chinese hamster ovary (CHO) animal cells. The lower concentration of titania in HAP produced less toxicity when compared to the increase in concentration and the cell was found to be more adhered to HAP. Hence, at the excess concentration, TiO₂ has better antibacterial activity against gram-positive bacteria and appeared to be bioactive.

Discussion

For the past few decades, the number of biocompatibility studies of biomaterials to understand its effect on cells

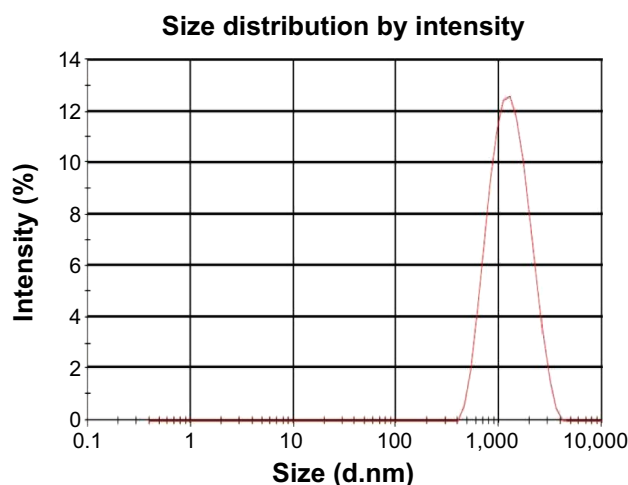


Figure 7 DLS analysis of TiO₂ powder sintered at 900°C for 2 hours in DMSO solvent.

Abbreviations: DLS, dynamic light scattering; TiO₂, titanium dioxide; DMSO, dimethyl sulfoxide.

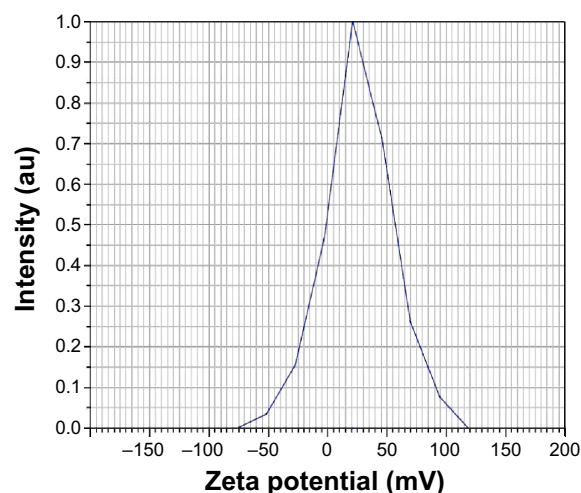


Figure 8 Zeta potential evaluation of TiO₂ powder sintered at 900°C for 2 hours in DMSO solvent.

Abbreviations: TiO₂, titanium dioxide; DMSO, dimethyl sulfoxide.

to produce better osteointegration has steadily increased. The cell viability depends on the prevailing environment in order to produce better cellular responses such as adhesion, cell viability, migration, proliferation. The biological effects steeply depend on the physicochemical properties of the prepared materials such as particle size, shape, surface area, phase purity, crystallite nature, and surface topography like surface charge properties as well as the concentration of particles.

However, Shi et al have published on the use of conventional TiO₂, their potential adverse effects, and beneficial activity. The effect of titania on different cell lines such as lung cells, nerve cells, cardiovascular cells, dermal and mucosal cells, and reproductive and renal cells was determined by several authors.³³ Nevertheless, from these studies excessively and unrealistically high doses, the size, shape, composition, crystalline nature, solubility, added functional groups and manufacturing impurities of these heterogeneous nature has been involved, and produces various conflicts of results for their effects on study material.

For instance, Sayes and Warheit³⁴ have studied the effect of different particle-sized rutile TiO₂ as surface coatings along with alumina and amorphous silica. In addition Sollazzo et al³⁵ have also shown the cell activity of crystalline phase composition of anatase TiO₂ coating on osteoblast MG63 cell lines. The results showed variations in the activity of genes with various functions, such as cell adhesion, proliferation, immunity, and lysosome composition, and furthermore, the study does not confirm any particle size distribution. Only limited studies of direct correlation of physicochemical properties of prepared materials with cell lines for its

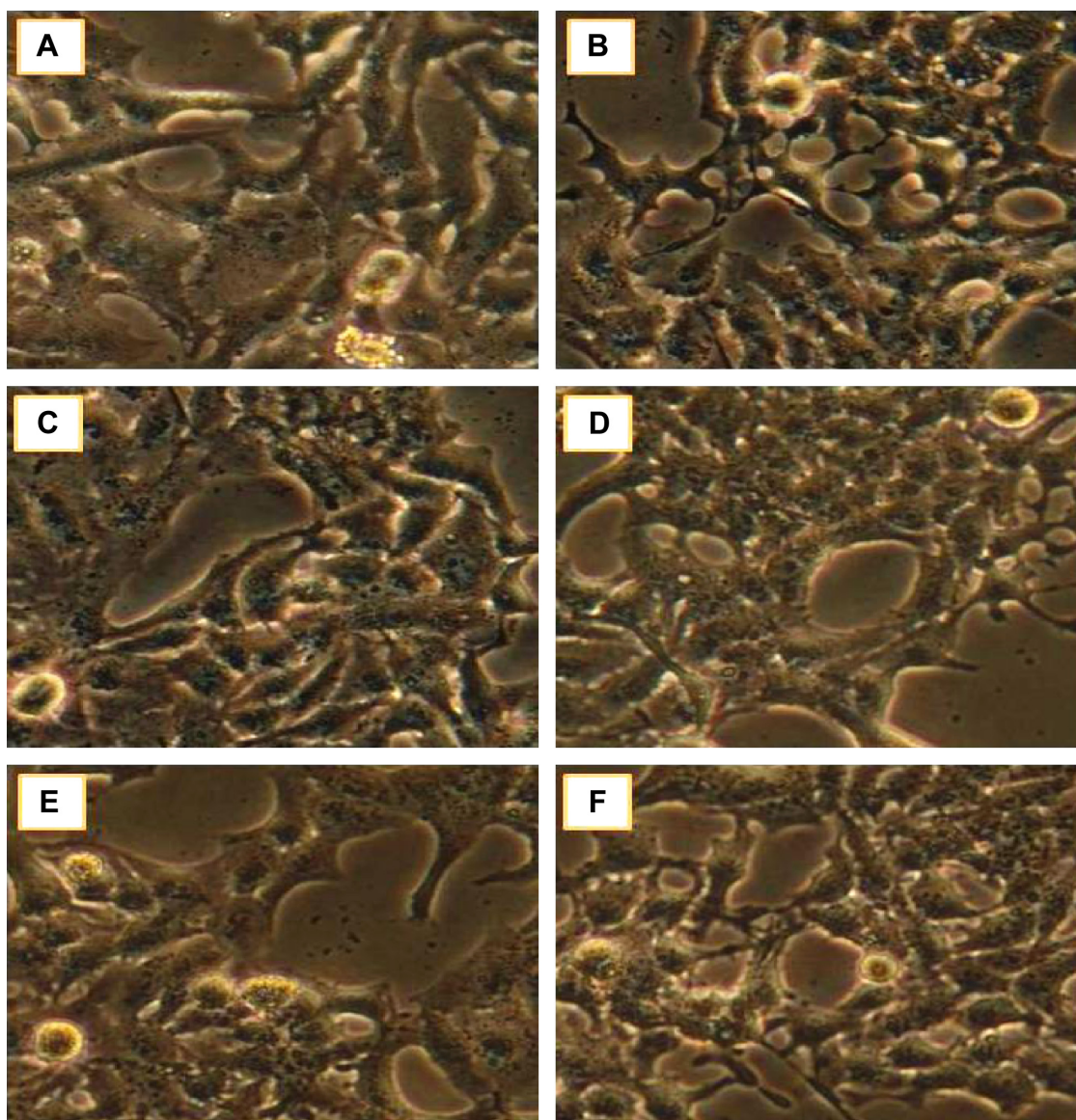


Figure 9 Cell viability/proliferation studies of synthesized TiO_2 nanoparticles on MG63 cell lines for 24-hour period.

Notes: (A) Control; (B) cell +1 $\mu\text{g/mL}$ of TiO_2 nanoparticles; (C) cell +10 $\mu\text{g/mL}$ of TiO_2 nanoparticles; (D) cell +25 $\mu\text{g/mL}$ of TiO_2 nanoparticles; (E) cell +50 $\mu\text{g/mL}$ of TiO_2 nanoparticles; (F) cell +100 $\mu\text{g/mL}$ of TiO_2 nanoparticles.

Abbreviation: TiO_2 , titanium dioxide.

biocompatibility effects were carried out. Braydich-Stolle et al³⁶ have studied the effect of size and crystal structure related to toxicity or mode of cell death. Gratton et al³⁷ confirmed the effects of nonspherical particle shape with absolute spherical size such as the rod-like particles are more easily and rapidly internalized than other particles shape.

Subsequently, Di Virgilio et al³⁸ evaluated the effect of polymorphic phase of anatase with different dose volume of 0–300 $\mu\text{g/mL}$ on rat osteosarcoma-derived cell lines. They found that an induction of cytotoxic effects and phagocytosed vesicles confirmed for osteointegration failure or toxicity of implanted materials. Martinez-Gutierrez et al³⁹ reported the

effect of combination of (anatase and rutile) TiO_2 phase with silver nanoparticles. They found that the combination of both the phases have shown excellent antifungal activity than the 100% rutile TiO_2 due to the possible intrinsic properties of the mineral composition.

This study has been carried out in order to further strengthen the effect of biocompatibility with respect to physicochemical characteristics of 100% rutile phase. The crystalline size of 114 nm having specific surface area of 12 m^2/g , zeta potential of 26.8 mV, and average hydrodynamic diameter of 1,140 nm with PDI value of 0.158 in DMSO of our sol-gel synthesized TiO_2 have been taken to

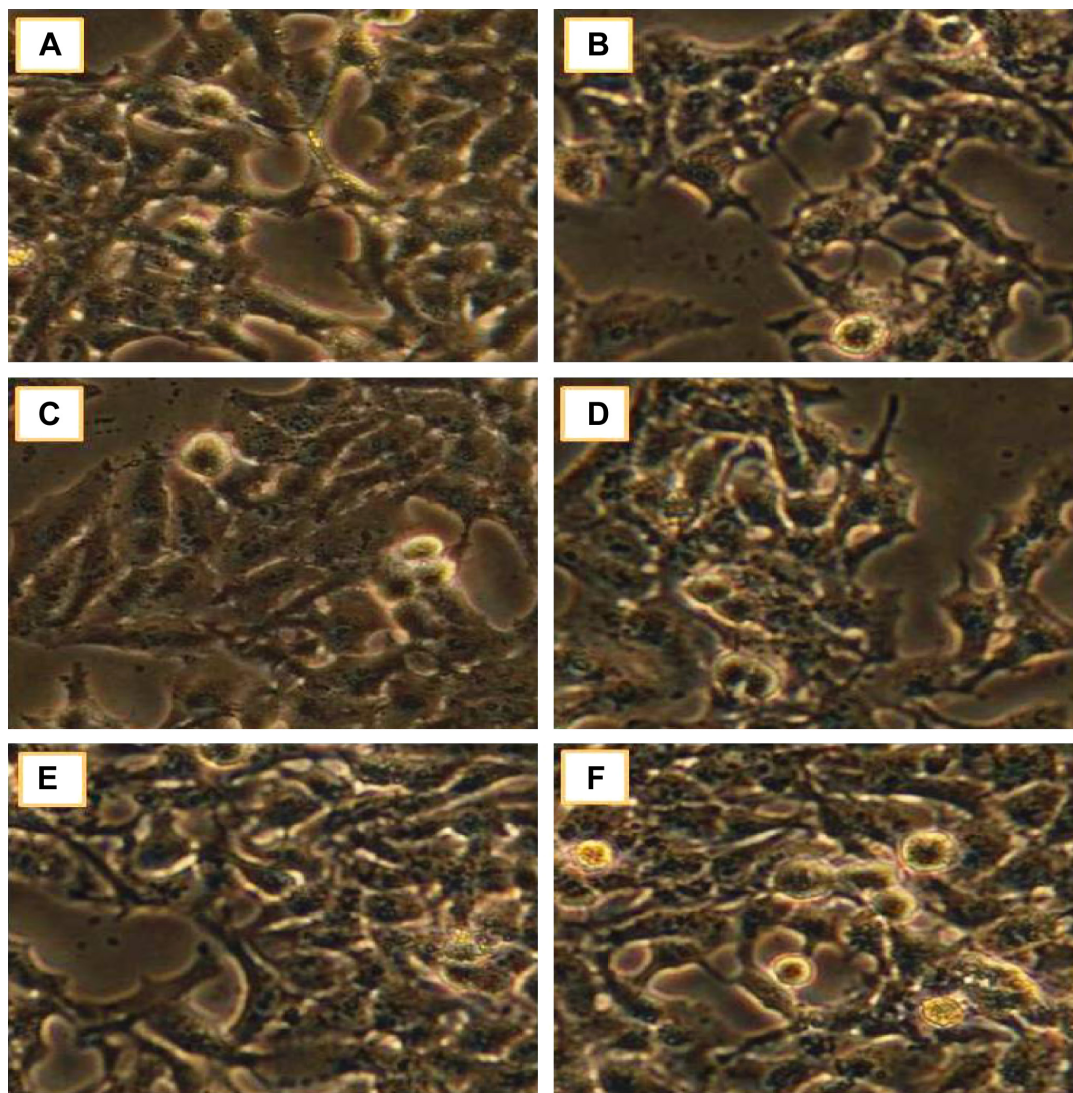


Figure 10 Cell viability/proliferation studies of synthesized TiO_2 nanoparticles on MG63 cell lines for 48-hour period.

Notes: (A) Control; (B) cell +1 $\mu\text{g/mL}$ of TiO_2 nanoparticles; (C) cell +10 $\mu\text{g/mL}$ of TiO_2 nanoparticles; (D) cell +25 $\mu\text{g/mL}$ of TiO_2 nanoparticles; (E) cell +50 $\mu\text{g/mL}$ of TiO_2 nanoparticles; (F) cell +100 $\mu\text{g/mL}$ of TiO_2 nanoparticles.

Abbreviation: TiO_2 , titanium dioxide.

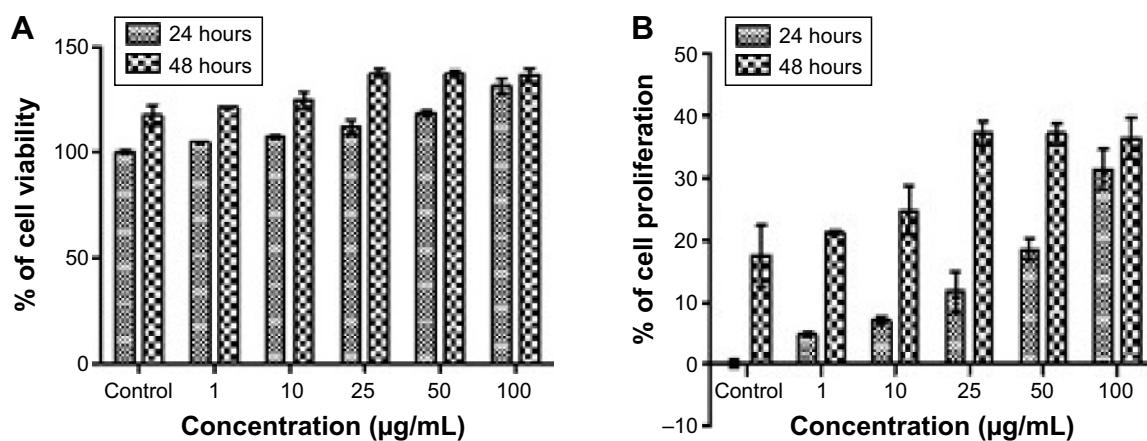


Figure 11 Shows osteoblast-like MG63 cell lines cell viability/proliferation.

Notes: (A) Cellular viability and (B) proliferation of MG63 cell lines treated with different concentrations of TiO_2 nanoparticles for 24 hour and 48 hour study period. Data are expressed as mean \pm standard error from three independent experiments.

Abbreviation: TiO_2 , titanium dioxide.

predict the biocompatibility with physiological body fluids for implantation as medical devices.

Our synthesized nano TiO_2 particles have better cell viability and proliferation without producing any toxicity, which confirms the biocompatibility in MG63 cell lines. This is due to the transformation of phase from anatase to rutile without other phases during sintering at 900°C for 2 hours. The rutile phase is a more inert phase than the highly active, high-refractive index anatase form of TiO_2 .⁴⁰ The prepared material shows an agglomerated platelet-like particle and not fiber-shaped particles and generally fiber-shaped particles are more reactive and toxic (such as carbon nanotubes, which are more toxic than fullerenes).^{41,42} Generally, phagocytic cells strongly interact with negatively charged particles than positively charged particles. The zeta potential value with positive sign indicates the prepared materials less susceptibility to phagocytic interaction.⁴³ From this, we can conclude that there is a possibility of better bioactive nature for producing osteointegration in bioimplant applications. The sample having characteristics of nanoparticle size distribution with 100% rutile polymorphic form has shown better biocompatibility. However, the validity of in vitro method results was affected by various internal and external factors. A detailed, in vivo study is needed to understand the cellular and molecular mechanism involved with different cell lines.

Conclusion

Pure TiO_2 nanoparticles were successfully synthesized by sol-gel technique with the prime objective of increasing the lifetime of biomedical devices such as implants and prostheses. The sintering temperature of 900°C for 2 hours produced less agglomerated nanoparticles with single-phase formation (rutile). The formed functional groups, phases and surface morphology, particle size, nature of hydrodynamic size (diameter) and its surface charge were confirmed by suitable characterization methods. The following conclusions can be drawn from the experiential methods described earlier as evidence:

- 1) The FT-IR and Powder XRD analytical techniques confirmed the presence of TiO_2 nanoparticles with characteristic functional groups and transformation of anatase to pure rutile phase during sintering process.
- 2) The nature of hydrodynamic size (diameter), surface charge, particle size, and morphological characteristics of prepared TiO_2 nanoparticles and their elemental compositions were justified by DLS analysis, zeta potential measurements, SEM-EDAX, and TEM analysis.

- 3) The simple, precise, and more accurate in vitro MTT biocompatibility assay was carried out on the prepared compound by using osteoblast MG63 cell lines, which have shown a stimulatory effect with increased cell growth and proliferation with different dose of a test material, ranging from $1\text{ }\mu\text{g/mL}$, $10\text{ }\mu\text{g/mL}$, $25\text{ }\mu\text{g/mL}$, $50\text{ }\mu\text{g/mL}$, to $100\text{ }\mu\text{g/mL}$ at different time periods of 24 hours and 48 hours. Among the doses of concentrations studied, a pronounced cell viability/proliferation was found to be observed in the dose or concentrations of $25\text{ }\mu\text{g/mL}$, $50\text{ }\mu\text{g/mL}$, and $100\text{ }\mu\text{g/mL}$ for the 48-hour duration. Hence, the prepared sample does not have cellular dysfunctionality but has enhanced cell viability and proliferation characteristics.

However, further experimental work has to be carried out to understand the cell toxicity on MG63 cell lines at a dose or concentration more than $100\text{ }\mu\text{g/mL}$ with different time periods. An in vivo study has to be performed for justification.

Acknowledgments

The authors thank the management of VIT University, Vellore, Tamil Nadu, for providing them an opportunity to carry out this work. The authors are grateful to Dr PS Suresh, Henry Ford Health System, USA, for reviewing the manuscript. They also thank Johnson & Johnson for sponsoring this study.

Disclosure

The authors report no conflicts of interest in this work.

References

1. Sridhar TM, Eliaz N, Mudali UK, Raj B. Electrophoretic deposition of hydroxyapatite coatings and corrosion aspects of metallic implants. *Corros Rev*. 2002;20(4-5):255-294.
2. Vijayalakshmi U, Rajeswari S. Development of silica glass coatings on 316L SS and evaluation of its corrosion resistance behavior in Ringer's solution. *Metall Mater Trans A*. 2012;43(12):4907-4919.
3. Vijayalakshmi U, Balamurugan A, Rajeswari S. Synthesis and characterization of porous silica gels for biomedical applications. *Trends Biomater Artif Organs*. 2005;18(2):101-105.
4. Pang XF. The physical and biological properties of nano TiO_2 material. *Mater Sci Appl*. 2011;2(7):940-945.
5. Geetha M, Durgalakshmi D, Asokamani R. Biomedical implants: corrosion and its prevention-A review. *Recent Pat Corro Sci*. 2010;2:50-54.
6. Nag S, Banerjee R. Fundamentals of medical implant materials. In: Narayan R, editor. *Materials for Medical Devices*. ASM Handbook; 2012:6-13.
7. Elshhawly W. Biocompatibility. In: Costas Sikalidis, editor. *Advances in Ceramics-Electric and Magnetic Ceramics, Bioceramics, Ceramics and Environment*. Intech; 2011:359-378.
8. Brunner TJ, Wick P, Manser P, et al. In vitro cytotoxicity of oxide nanoparticles: comparison to asbestos, silica, and the effect of particle solubility. *Environ Sci Technol*. 2006;40(14):4734-4781.

9. Roach P, Eglin D, Rohde K, Perry CC. Modern biomaterials: a review-bulk properties and implications of surface modifications. *J Mater Sci Mater Med*. 2007;18(7):1263–1277.
10. Kokubo T, Kim H-M, Kawashita M. Ceramics for biomedical applications. In: Somiya S, Aldinger F, Claussen N, et al, editors. *Hand Book of Advanced Ceramics, Vol II Processing and Their Applications*. London: Academic Press; 2003:385–413.
11. Karlsson HL, Cronholm P, Gustafsson J, Moller L. Copper oxide nanoparticles are highly toxic: a comparison between metal oxide nanoparticles and carbon nanotubes. *Chem Res Toxicol*. 2008;21(9):1726–1732.
12. Jennifer M, Maciej W. Nanoparticle technology as a double-edge sword: cytotoxic, genotoxic and epigenetic effects on living cells. *J Biomater Nanobiotechnol*. 2013;4:53–63.
13. Moschini E, Gualtieri M, Gallinotti D, et al. Metal oxide nanoparticles induce cytotoxic effects on human lung epithelial cells A549. *Chem Eng Trans*. 2010;22:29–34.
14. St Pierre CA, Chan M, Iwakura Y, Ayers DC, Kurtjones EA, Finberg RW. Periprosthetic osteolysis: characterizing the innate immune response to titanium wear-particles. *J Orthop Res*. 2010;28(11):1418–1424.
15. Xiong S, George S, Yu H, et al. Size influences the cytotoxicity of poly(lactic-co-glycolic acid (PLGA) and titanium dioxide (TiO₂) nanoparticles. *Arch Toxicol*. 2013;87(6):1075–1086.
16. Sayes CM, Wahi R, Kurian PA, et al. Correlating nanoscale titania structure with toxicity: a cytotoxicity and inflammatory response study with human dermal and fibroblasts and human lung epithelial cells. *Toxicol Sci*. 2006;92(1):174–185.
17. Wang JX, Fan YB, Gao Y, Hu QH, Wang TC. TiO₂ nanoparticles translocation and potential toxicological effect in rats after intraarticular injection. *Biomaterials*. 2009;30:4590–4600.
18. Qiang ZX, Hong YL, Meng T, Pu PY. ZnO, TiO₂, SiO₂ and Al₂O₃ nanoparticles induced toxic effects on human fetal lung fibroblast. *Biomed Environ Sci*. 2011;24(6):661–669.
19. Hou Y, Cai K, Li J, et al. Effects of titanium nanoparticles on adhesion, migration, proliferation and differentiation of mesenchymal stem cells. *Int J Nanomedicine*. 2013;8:3619–3630.
20. Lai JC, Lai MB, Jandhyam S, et al. Exposure to titanium dioxide and other metallic oxide nanoparticles induces cytotoxicity on human neural cells and fibroblasts. *Int J Nanomedicine*. 2008;3(4):533–545.
21. Ekwall B, Silano V, Stammati P, Zucco F. Toxicity tests with mammalian cell cultures. In: Bourdeau P, et al, editors. *Short-Term Toxicity Tests for Non-Genotoxic Effects*. New York: Chichester; 1990:75–97.
22. Huang J, Di Silvio L, Wang M, Rehman I, Ohtsuki C, Bonfield W. Evaluation of in vitro bioactivity and biocompatibility of bioglass[®]-reinforced polyethylene composite. *J Mater Sci Mater Med*. 1997;8(12):809–813.
23. Javicoli I, Leso V, Fontana L, Bergamaschi A. Toxicological effects of titanium dioxide nanoparticles: a review on *in-vitro* mammalian studies. *Eur Rev Med Pharmacol Sci*. 2011;15(5):481–508.
24. Palanivelu R, Rubankumar A. Synthesis and spectroscopic characterization of hydroxyapatite by sol-gel method. *Int J Chem Tech Res*. 2013;5(6):2965–2969.
25. Hamadian M, Reisi-Vanani A, Majedi A. Sol-gel preparation and characterization of Co/TiO₂ nanoparticles: application to the degradation of methyl orange. *J Iran Chem Soc*. 2010;7(suppl 2):S52–S58.
26. Mohan L, Durgalakshmi D, Geetha M, Sankaranarayan TSN, Asokamani R. Electrophoretic deposition of nanocomposite (Hap+TiO₂) on titanium alloy for biomedical applications. *Ceram Int*. 2012;38(4):3435–3443.
27. Lin CK, Yang TJ, Feng YC, Tsung TT, Su CY. Characterization of electrophoretically deposited nanocrystalline titanium dioxide films. *Surf Coat Technol*. 2006;200:3184–3189.
28. Chang JA, Vithal M, Baek IC, Seok SI. Morphological and phase evolution of TiO₂ nanocrystals prepared from peroxotitanate complex aqueous solution: influence of acetic acid. *J Solid State Chem*. 2009;182:749–756.
29. Gai L, Mei Q, Qin X, Li W, Jiang H, Duan X. Controlled synthesis of anatase TiO₂ octahedra with enhanced photo catalytic activity. *Mater Res Bull*. 2013;48:4469–4475.
30. Chaudhary V, Srivastava AK, Kumar J. On the sol-gel synthesis and characterization of titanium dioxide nanoparticles. *Mater Res Soc Symp Proc*. 2011;1352:10–24.
31. Zhang Y, Yang M, Portney NG, et al. Zeta potential: a surface electrical characteristic to probe the interaction of nanoparticles with normal and cancer human breast epithelial cells. *Biomed Microdevices*. 2008;10:321–328.
32. Nathanael AJ, Mangalaraj D, Hong SI. Biocompatibility and antimicrobial activity of hydroxyapatite/titania bio-nanocomposite. In: 18th International Conference on Composite Materials (ICCM 2011); Aug 21–26, 2011; Jeju Island, Korea.
33. Shi H, Magaye R, Castranova V, Zhao J. Titanium dioxide nanoparticles: a review of current toxicological data. *Part Fibre Technol*. 2013;10(15):1–33.
34. Sayes CM, Warheit DB. An in vitro investigation of the differential cytotoxic responses of human and rat lung epithelial cell lines using TiO₂ nanoparticles. *Int J Nanotechnol*. 2008;5(1):15–29.
35. Sollazzo V, Palmieri A, Pezzetti F, et al. Genetic effect of anatase on osteoblast-like cells. *J Biomed Mater Res B Appl Biomater*. 2008;85(1):29–36.
36. Braydich-Stolle LK, Schaublin NM, Murdock RC, et al. Crystal structure mediates mode of cell death in TiO₂ nanotoxicity. *J Nanopart Res*. 2009;11:1361–1374.
37. Gratton SE, Ropp PA, Pohlhaus PD, et al. The effect of particle design on cellular internalization pathways. *Proc Natl Acad Sci U S A*. 11618;105(33):11613–11618.
38. Di Virgilio AL, Reigosa M, De Mele MF. Response of UMR 106 cells exposed to titanium oxide and aluminium oxide nanoparticles. *J Biomed Mater Res A*. 2010;92(1):80–86.
39. Martinez-Gutierrez F, Olive PL, Banuelos A, et al. Synthesis, characterization and evaluation of antimicrobial and cytotoxic effect of silver and titanium nanoparticles. *Nanomedicine*. 2010;6:681–688.
40. Wang J, Fan Y. Lung injury induced by TiO₂ nanoparticles depends on their structural features: size, shape, crystal phases and surface coating. *Int J Mol Sci*. 2014;15:22258–22278.
41. Gattoo MA, Naseem S, Arfat MY, Dar AM, Qasim K, Zubair S. Physicochemical properties of nanomaterials: implication in associated toxic manifestations. *Biomed Res Int*. 2014;2014:498420.
42. Hsiao I, Huang Y. Effects of various physicochemical characteristics on the toxicities of ZnO and TiO₂ nanoparticles toward human lung epithelial cells. *Sci Total Environ*. 2011;409(7):1219–1228.
43. Frolich E. The role of surface charge in cellular uptake and cytotoxicity of medical nanoparticles. *Int J Nanomedicine*. 2012;7:5577–5591.

International Journal of Nanomedicine

Publish your work in this journal

The International Journal of Nanomedicine is an international, peer-reviewed journal focusing on the application of nanotechnology in diagnostics, therapeutics, and drug delivery systems throughout the biomedical field. This journal is indexed on PubMed Central, MedLine, CAS, SciSearch®, Current Contents®/Clinical Medicine,

Submit your manuscript here: <http://www.dovepress.com/international-journal-of-nanomedicine-journal>

Journal Citation Reports/Science Edition, EMBase, Scopus and the Elsevier Bibliographic databases. The manuscript management system is completely online and includes a very quick and fair peer-review system, which is all easy to use. Visit <http://www.dovepress.com/testimonials.php> to read real quotes from published authors.